ACS Photonics

Letter

pubs.acs.org/journal/apchd5

Nonperturbative Hydrodynamic Model for Multiple Harmonics Generation in Metallic Nanostructures

Pavel Ginzburg,*[,†,‡,§] Alexey V. Krasavin,[†,§] Gregory A. Wurtz,[†] and Anatoly V. Zayats[†]

[†]Department of Physics, King's College London, Strand, London WC2R 2LS, United Kingdom

[‡]ITMO University, St. Petersburg 197101, Russia

ABSTRACT: The electromagnetic response of a free-electron gas leads to the inherent nonlinear optical behavior of nanostructured plasmonic materials enabled through both strong local field enhancements and complex collective electron dynamics. Here, a time-domain implementation of the hydrodynamic model for conduction electrons in metals has been developed to enable nonperturbative studies of nonlinear coherent interactions between light and plasmonic nanostructures. The effects originating from the convective acceleration, the magnetic contribution of the Lorenz force, the quantum electron pressure, and the presence of the nanostructure's boundaries have been taken into account, leading to the appearance of both second and third harmonics. The proposed time-domain method enables obtaining a universal, self-consistent numerical solution, free from any approximations, allowing investigations of nonlinear optical interactions with arbitrary spatially and temporally shaped optical pulses, opening unique opportunities to approach description of realistic experimental scenarios.

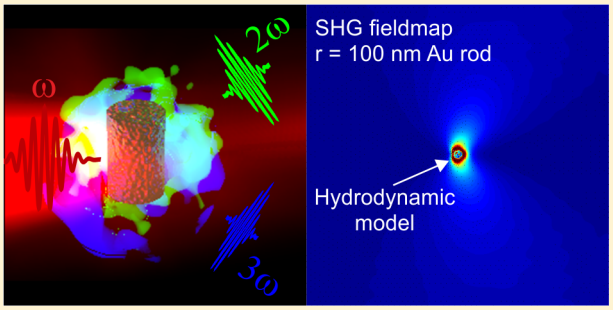

KEYWORDS: *plasmonics, nonlinear optics*

Nonlinear optical interactions give rise to a variety of phenomena extensively used in numerous applications in lasers, classical and quantum optical information processing, bioimaging, and sensing. Consequently, tailoring, enhancing, and controlling nonlinear processes, which are inherently weak and require high light intensities, is a task of prime importance. One approach offering promising developments in this area employs nanostructured materials to tailor enhanced effective nonlinear susceptibilities through geometrical means by shaping local electromagnetic fields.

Plasmonic nanostructures deliver both true nanoscale light confinement and strong nonlinear response, as both rely on peculiarities of the response of conduction electrons to the electromagnetic field of incident light.[1] Both second and third harmonics generation (SHG and THG), optical Kerr nonlinearities, and the possibility to achieve solitonic waves have been demonstrated via the coupling to plasmonic resonances in metal films and metallic nanostructures.[2−6] Typical theoretical approaches used in the description of the nonlinear response of plasmonic materials rely on a perturbative treatment of the material's polarization, either through a hydrodynamic model or phenomenologically, enabling the filtering of the nonlinear harmonic fields generated via a quasi-Fourier transformation.[7]

In this Letter, we develop a comprehensive and nonperturbative numerical model for the investigation of nonlinear interactions of light with plasmonic nanostructures. The complete time-domain analysis fully addresses the nonlinear dynamics of free electrons without any additional assumptions on the nature of the interaction, providing the opportunity to explore the interplay between various nonlinear optical processes. The optical properties of metal particles are described with the help of a full hydrodynamic model,[8] which enables accounting for both linear and nonlinear dynamics of the conduction electrons under visible and infrared light illumination, away from the spectral range of interband transitions. While the hydrodynamic equations straightforwardly reproduce the Drude model in the linear regime of interaction with electromagnetic fields, at higher intensities, convective acceleration, magnetic contributions from the Lorenz force, and quantum electron pressure terms, present in the hydrodynamic model, introduce strong nonlinear contributions to the optical response of the system. Time-domain studies give an opportunity to explore simultaneously both bulk and surface contributions to nonlinear generation processes, as well as the efficiency of sideband generation. All these effects have simultaneously been taken into account by coupling nonlinear hydrodynamic equations, describing the behavior of the electron plasma, with Maxwell's equations to model the response to electromagnetic fields. As a model example, we analyze the nonlinear scattering from a gold nanocylinder. Our theoretical approach allows the observation of third-harmonic radiation as well as boundary-enabled second-harmonic responses.[9] As will be shown here, clear differences emerge when comparing the results obtained from the hydrodynamic formulation with the phenomenological

Received: October 2, 2014
Published: December 12, 2014

model, in both the properties of nonlinear harmonic generation and the associated radiation pattern. These differences are discussed and reinforce the importance of using the presented approach in the nonlinear optical study of nanoscale objects. Moreover, it will be shown that frequently used approximated models should be reconsidered. No approximations on the pulse shape and the time dependence of electromagnetic fields were made in the model, applicable unless the hydrodynamic description of the metal breaks down, e.g., for very short time scales not addressed here. The presented approach also enables studying carrier envelop phase effects and other ultrafast interaction dynamics.[10]

Self-Consistent Formulation of the Electromagnetic−Hydrodynamic Problem. The interaction of electromagnetic fields with objects made from arbitrary (nonmagnetic) materials is described in terms of the induced polarization $\vec{P}$ via the wave equation

$$\nabla \times \nabla \times \vec{E}(\vec{r}, t) + \frac{1}{c^2}\partial_{tt}\vec{E}(\vec{r}, t) + \mu_0 \partial_{tt}\vec{P}(\vec{r}, t) = 0 \tag{1}$$

where $\vec{E}(\vec{r},t)$ is the electric field, c is the speed of electromagnetic waves in a vacuum, and μ_0 is the vacuum permeability. In general, the coordinate-dependent polarization term contains all the information on both linear and nonlinear contributions, also including chromatic dispersion. In the framework of the hydrodynamic model, $\vec{P}$ is introduced via polarization currents, which are defined with the help of natural hydrodynamic variables: the macroscopic position-dependent electron density $n(\vec{r},t)$ and velocity $\vec{v}(\vec{r},t)$. The basic set of hydrodynamic equations is then given by[8]

$$\begin{aligned} &m_e n(\partial_t \vec{v} + \vec{v}\cdot\nabla\vec{v}) + \gamma m_e n\vec{v} = -en(\vec{E} + \vec{v} \times \vec{H}) - \vec{\nabla}p \\ &\partial_t n + \nabla\cdot(n\vec{v}) = 0 \end{aligned} \tag{2}$$

where m_e and e are the electron mass and charge, respectively, γ is the effective scattering rate, representing optical losses in a phenomenological way, and $p = (3\pi^2)^{2/3}(\hbar^2/5m_e)n^{5/3}$ is the quantum pressure evaluated within the Thomas−Fermi theory of an ideal Fermionic gas. The $\vec{v}\cdot\nabla\vec{v}$ term is the convective acceleration (in analogy to fluid dynamics) and is one of the key contributors to the nonlinear harmonic generation process. The electromagnetic (eq 1) and hydrodynamic (eq 2) sets of equations are coupled via the microscopic polarization term

$$\partial_t \vec{P} = -en\vec{v} \tag{3}$$

Equations 1−3 provide a self-consistent formulation of nonlinear optical processes originating from free conduction electrons in plasmonic systems. The effects of both surface nonlinearities and nonlocality are taken into account via the boundary conditions imposed by Maxwell's equations and vanishing current perpendicular to the boundaries. The proposed approach is a new nonperturbative description of free-electron nonlinearities allowing accounting for all hydrodynamic processes of the electron plasma. It is worth noting that, to the best of our knowledge, all previous studies addressed only linear, single-frequency regimes, while nonlinear contributions were taken into account perturbatively via quasi-Fourier transform techniques.

Details of the Numerical Model. While the proposed method is universal and enables addressing any geometry, here, as a particular example, the problem of nonlinear scattering of TM plane waves by an infinitely long cylinder of nanoscale diameter is considered (Figure 1). The simulation domain

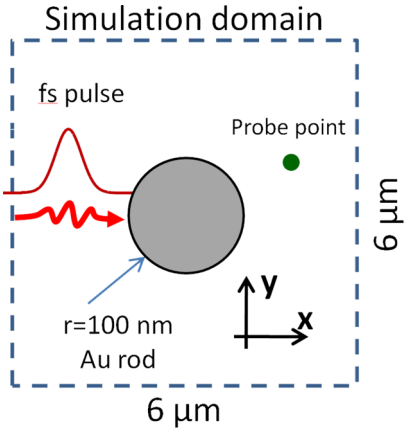

Figure 1. Simulation layout of nonlinear optical generation from a gold cylinder illuminated by a short pulse.

includes both near- and far-field regions, thus taking into account possible field enhancements in the near-field of the nanoparticle. This will allow for a comparison of our results to other known approaches developed for metal nanoparticles. Tabulated physical constants were used for the implementations of eqs 1−3, and the constants for gold were taken to be $n_0 = 5.98 \times 10^{28}$ m^{-3}, $\gamma = 1.075 \times 10^{14}$ s^{-1}, and $\omega_p = 9.0834$ eV. In the linear regime, eqs 2 and 3 provide the general Drude-like response of the electron gas. This was numerically tested by comparing the low-intensity linear scattering in the full hydrodynamic model with the linear scattering simulated as when the Drude response is conventionally introduced via the dielectric permittivity. The nonlinear terms in the full hydrodynamic model become significant only under high-intensity excitation.

The set of eqs 1−3 was numerically solved by employing the finite element method. A Gaussian pulse of the form $\vec{E}^{\omega}(y,t) = (0,E_y^{\omega})\ \exp[-\ y^2/(2w^2)]\ \exp[-(t\ -\ t_0)^2/(2\tau^2)]\ \cos[\omega t]$ was considered at the fundamental driving frequency of $\omega = 1.257 \times 10^{15}$ rad/s, corresponding to a free-space wavelength of $\lambda = 1500$ nm (≈0.83 eV), with a temporal width τ and a spatial width $w = \lambda/2$. The pulse has a linear polarization in the y-direction and is incident on the metal cylinder of radius $r = 100$ nm along the x-direction (Figure 1). The time offset $t_0 = -3\tau$ and simulation time span $T = 7\tau$ were chosen so that the scattered light pulse containing higher harmonics is able to entirely propagate across the 6×6 μm^2 simulation domain. Additionally, it was checked that any further increase of the simulation time span does not affect the results. A maximum peak intensity of $I_0^{\omega} = 9 \times 10^{18}$ W/m^2, corresponding to a typical intensity the particle can still withstand due to surface-induced ablation effects[11] (with the correction for the incident light wavelength), was used to ensure convergence of the model, for any experimentally relevant intensity.

Nonlinear Spectrum. The time dependence of the nonlinear scattered signal obtained after subtracting the linear scattered excitation field was probed in the near and far field regions. Subsequently, it was Fourier transformed in the frequency domain exhibiting typical multiple harmonics spectra (Figure 2a). For a very short pulse ($\tau = 5$ fs), the separation between harmonics is comparable to their spectral width and shows the overlap between second and third harmonics (SH

dx.doi.org/10.1021/ph500362y | ACS Photonics 2015, 2, 8−13

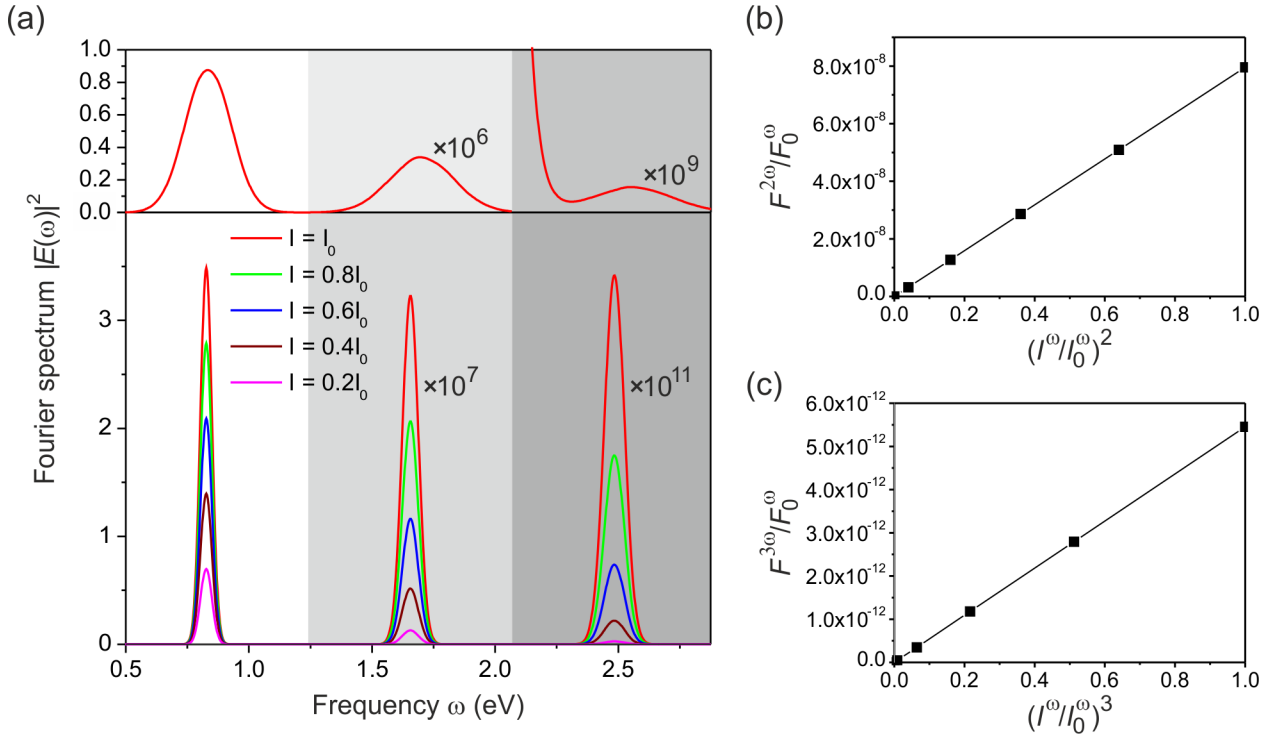

Figure 2. (a) Nonlinear scattering spectra from the infinitely long Au cylinder of 100 nm radius simulated for the excitation pulse of τ = 5 fs (top) and τ = 20 fs (bottom). (b, c) Integrated flux $F^{2\omega}$ for (b) SHG and (c) THG normalized to the maximum incident fundamental flux F_0^{ω} (corresponding to the peak intensity I_0^{ω}) as a function of the fundamental light intensity.

and TH) spectra (Figure 2a, top panel). For longer excitation pulses (τ = 20 fs), nonlinear harmonics are well separated (Figure 2a, bottom panel). The spectral widths of the SH and TH signals are larger than those of the fundamental pulse, as the temporal nonlinear pulses are shorter due to the nonlinear dependence on the excitation field. For further comparison, the pump pulse energy at both pulse widths was normalized. As a result, the peak intensity for the τ = 5 fs pulse is larger than that observed for τ = 20 fs pulse, leading to an increased ratio between TH and SH intensities for the shorter pulse. In the short-pulse excitation regime, a small (several tens of nm) blue shift of both SH and TH peaks is observed with respect to the respective harmonics of the central fundamental frequency. This is due to the dispersion of the imaginary part of the frequency-dependent permittivity of Au.

The power dependence of the nonlinear harmonic generation was determined via the spectral dependence of the far-field intensity $|E(\omega)|^2$ integrated over the harmonic spectra to extract the relative intensities of the nonlinear signals. The latter were then integrated over a cylindrical surface of radius 2λ centered on the rod to obtain the total fluxes of the generated harmonics. As a crucial proof of the validity of the model, it was found that those dependencies follow the well-defined powers of the pump, quadratic and cubic for SH and TH, respectively, as expected for nonlinear optical processes (Figure 2b,c). Since the THG intensity grows with the third power of the fundamental intensity and SHG with the second, the former shows comparably faster growth with the excitation intensity (Figure 2a). The same results are obtained for different integration cylinder radii of λ and $3/2\lambda$, confirming that the integration was performed in the radiation zone. From the slopes of the dependences one can evaluate the effective nonlinear susceptibilities of the Au nanorod to be $\chi^{(2)} \approx 10^{-13}$ m/V and $\chi^{(3)} \approx 10^{-26}$ m^2/V^2. The $\chi^{(3)}$ value is consistent with the nonlinear susceptibility of Au examined in ref 12 taking into account fundamental-pulse duration and wavelength, while the second-order susceptibility, although strongly geometry-dependent, is of a value that is also typical for nanostructured objects.

Second Harmonic Generation. A frequency domain analysis of the hydrodynamic equations allows deriving surface polarizabilities[9] for a particle under the undepleted pump assumption. The effective nonlinear surface polarizability can also be introduced phenomenologically and related to the experimental data. The SHG from nanoparticles was intensively studied in the quasistatic limit[13,14] as well as relying on the extended Mie theory[15,16] with one of the central points being to account for nonlocal and retardation effects responsible for the radiation pattern formation. Advanced numerical modeling carried out in the frequency domain enables addressing arbitrary particle geometries,[17] but restricted to an a priori chosen model for the nonlinear response.

In order to compare our time-domain approach to existing models, we have studied the second-harmonic radiation pattern calculated with the help of our full hydrodynamic description (Figure 3a). The SH intensity distribution was calculated by spectral frequency filtering and represents the intensity $|E(\omega)|^2$ of the SH signal at each simulation domain point integrated over the spectral spread of the SH resonance. The emission diagram has two radiation lobes pointing predominantly in the vertical (y-) direction and showing the appearance of a modified dipole radiation. It is worth noting that in the chosen geometry, we can identify the main contribution to the SHG from the convective acceleration and the Lorenz force with comparable contributions, while the quantum pressure effects, expected to result in 5/3 harmonic generation, were not

dx.doi.org/10.1021/ph500362y | ACS Photonics 2015, 2, 8−13

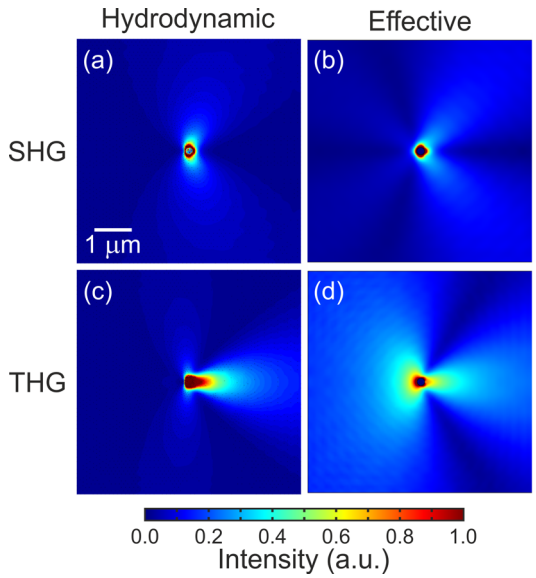

Figure 3. Intensity distributions of the nonlinear scattering around the infinitely long Au cylinder of 100 nm radius simulated for the excitation pulse of τ = 20 fs for (a, b) SHG and (c, d) THG in (a, c) microscopic hydrodynamic and (b, d) phenomenological effective models. The color scale is internal for each plot.

observed (the quantum pressure term enters eq 2 and is proportional to the carrier concentration in the power of 5/3; hence the appearance of a fractional harmonic might be expected). Note that the relative contribution of the different terms may differ depending on a particular geometry.

To compare this radiation pattern to that obtained from a phenomenological model, Figure 3b shows the SH radiation pattern evaluated using a two-step model, in which the fundamental field inside the particle is calculated in a first step and the nonlinear field distribution is subsequently derived in a second step using a source of the surface nonlinear polarization $P^{2\omega}_{\mathrm{surf},\perp} = \chi_{\mathrm{surf},\perp\perp\perp}(E^{\omega}_{\mathrm{pump},\perp})^2$, where $\perp$ stands for the local normal to the surface.[17] This assumes the nondepleted pump regime, relies on a quasi-Fourier separation of the harmonics, and makes the explicit restricting assumption on the interaction nature to originate from local boundary terms only. The latter follows from the centrosymmetric nature of considered particle's material, so that the dipolar SH radiation from the bulk is forbidden by the selection rules. In this case, one can clearly observe four lobes determined by a quadrupole-like emission added to a dipolar (two lobes) contribution. The phase relations between the two contributions determine the directivity of total SH emission. One can see the similarities of the nonperturbative and phenomenological models (cf. Figure 3a and b); however, the ratio between the dipolar and quadrupolar contribution is heavily distorted in favor of the latter in the phenomenological model. The phenomenologicaly defined surface polarization term also results in an unphysical singularity at the boundary, failing to describe the near-field distribution of the nonlinear source; conversely, the full time-domain method reproduces the physics of surface interactions with much better accuracy in both near- and far-field regions.

Third Harmonic Generation. Bulk third-harmonic generation in metals has been considered by the introduction of a nonlocal ponderomotive force, acting on electrons subjected to an electromagnetic field gradient.[18] Higher-harmonic generation at boundaries (e.g., flat metal surfaces), based on the Sommerfeld free-electron models with subsequent solution of the Schrödinger equation in the Kramers−Henneberger accelerating frame, were also developed[19] and are in good agreement with experimental data.[20] However, the impact of complex geometries on higher-harmonic generation is virtually not studied to date, primarily due to both experimental difficulties and the complex theoretical treatment required. The method developed here enables efficiently addressing this theoretical challenge.

The TH radiation pattern generated by the nanorod (Figure 3c) possesses strong beaming characteristics in the forward scattering direction as expected for large particles, for which retardation effects lead to constructive interferences in the forward direction only, lowering the backward scattered intensity.[21] In order to perform a comparison between the time-domain approach and phenomenological model, the TH intensity distribution was simulated with the above-described two-step model using a nondispersive, bulk third-order susceptibility. The radiation pattern derived phenomenologically has similar features to the microscopic model with a stronger backward THG (Figure 3d). The same as for the SHG pattern, strong differences are observed in the near field of the nanocylinder; while the phenomenological model assumes a third-order susceptibility to be homogeneous across the nanorod, the differences between models may be indicative of a position-sensitive effective third-order susceptibility arising from the hydrodynamic description.

For the geometry and the pump powers considered here, the signature of the fourth harmonic has been reliably observed, but higher harmonics are beyond the numerical accuracy of the simulations.

Resonance Effects. By tuning the nanoparticle geometry, the spectrum of its resonances can be engineered on demand.[22,23] This leads to enhanced electromagnetic fields and scattering, and the combination of various resonant conditions at both fundamental and harmonic frequencies can be used to significantly modify the nonlinear scattering.[1] Even at moderate illumination intensities, resonant effects start to be especially important in small metal nanostructures, as they enhanced the effective nonlinear surface response.[24] In order to study the impact of localized surface plasmon (LSP) resonances at either fundamental or nonlinear harmonic frequencies, either the particle shape or material can be modified.[25] We have chosen to change the electron concentration of the metal while keeping the particle geometry and dimensions the same, in order to obtain a plasmonic dipolar resonance in free space ($\varepsilon_{\mathrm{metal}} = -1$) at either the fundamental, second, or third harmonic frequencies. This allows us to compare the effects of the resonant field enhancement while not significantly influencing the carrier distribution $n(r)$ within the particle, which would be the case for varying geometry. It should be noted, however, that changing the electron density influences not only the plasma frequency but also the nonlinear susceptibilities (eq 1).[17] The nonlinear generation efficiency—the parameter that depends on the $\chi^{(2)}$ and $\chi^{(3)}$ of the medium as well as the excitation conditions—was evaluated in all the studied cases via a numerical estimation of the slopes on power-dependent graphs similar to those in Figure 2b,c. The enhancements were calculated relative to the geometry considering the natural electron concentration described above.

Both second and third harmonics show the highest enhancements, 5 and 10 orders of magnitude, respectively, for the 20 fs excitation pulse, when the nanocylinder has a LSP

dx.doi.org/10.1021/ph500362y | ACS Photonics 2015, 2, 8−13

resonance at the fundamental frequency. For the LSPs at the SH frequency, the observed enhancement is 4 and 6 orders of magnitude, and at the TH frequency, it is 2 and 5 orders of magnitude for SHG and THG efficiencies, respectively. For all the LSP resonances, the ratio between TH and SH intensities increases, so that at the fundamental LSP frequency TH intensity is 1 order of magnitude higher than the SH intensity at the highest fundamental intensity studied, with comparable TH and SH intensities for other resonant cases, in contrast to the nonresonant situation where SHG dominates. This indicates the stronger importance of the excitation field enhancement over the increased scattering cross-section of the nonlinear harmonics. At the fundamental frequency resonance, the effective "enhanced" susceptibility corresponds to $\chi^{(2)} \approx 10^{-10}$ m/V and $\chi^{(3)} \approx 10^{-21}$ m^2/V^2. Taking into account that these were obtained with the reduced electron concentration $(n/n_0 = 60)$, the effective nonlinearity of Au nanoparticles in these resonant conditions may be comparable to the best nonlinear dielectrics, even under femtosecond excitation.

In conclusion, we presented a comprehensive time-domain treatment of the microscopic polarization of conduction electrons using a full hydrodynamic description allowing for a self-consistent modeling of both the linear and nonlinear response of plasmonic nanostructures including the generation of multiple harmonics. The effects originating from the convective acceleration, the magnetic contribution of the Lorenz force, the quantum electron pressure, and the presence of the nanostructure's boundaries have been taken into account, leading to the appearance of both second and third harmonics. The developed method provides an ultimate approach to investigate the nonlinear response of arbitrarily shaped complex nanoscale plasmonic structures and enables addressing their self-consistent nonlinear dynamics. While various approaches typically make restricting assumptions on the nonlinear dynamics, such as undepleted pump or uncoupled frequencies approximations, in order to simplify the solutions of the coupled nonlinear equations, the proposed method enables one to obtain a universal, self-consistent numerical solution, free from any approximations. Moreover, it should be emphasized that the straightforward perturbative hydrodynamic description (e.g., relying on phenomenological second-order polarizability) is inconsistent with the full model reported here, underlining the fact that the majority of previously employed approaches should be reconsidered. Furthermore, nanostructures with arbitrary geometry and resonant frequencies for excitation, nonlinear scattering, or both can be comprehensively studied using the proposed model. The developed nonperturbative model enables investigating a vast number of multidisciplinary problems, involving metal composites interacting with weak, moderate, or intense optical pulses. The role of nonlocal electromagnetic response,[26] the effects accounting for the response of core electrons,[27] and employing quantum approaches for electron exchange correlations[28] can also be straightforwardly included.[29] Furthermore, the developed formalism paves the way for investigating ultrafast dynamics in mesoscopic and nanoscopic systems with properties defined via microscopic degrees of freedom, which can be introduced in the permittivity model.

AUTHOR INFORMATION

Corresponding Author

*E-mail: pavel.ginzburg@kcl.ac.uk.

Author Contributions

[§]P. Ginzburg and A. V. Krasavin contributed equally.

Notes

The authors declare no competing financial interest.

ACKNOWLEDGMENTS

This work has been supported, in part, by EPSRC (UK). A.Z. acknowledges support from the Royal Society and the Wolfson Foundation. P.G. and A.Z.'s work was supported by the U.S. Army Research Office. G.W. is grateful for support from the People Programme (Marie Curie Actions) of the EC FP7 project 304179. The authors are thankful to Michael Scalora for the discussions.

REFERENCES

(1) Kauranen, M.; Zayats, A. V. Nonlinear plasmonics. *Nat. Photonics* **2012**, *6*, 737−748.

(2) Wokaun, A.; Bergman, J. G.; Heritage, J. P.; Glass, A. M.; Liao, P. F.; Olson, D. H. Surface second-harmonic generation from metal island films and microlithographic structures. *Phys. Rev. B* **1981**, *24*, 849−856.

(3) Kim, E. M.; Elovikov, S. S.; Murzina, T. V.; Nikulin, A. A.; Aktsipetrov, O. A.; Bader, M. A.; Marowsky, G. Surface-enhanced optical third-harmonic generation in Ag island films. *Phys. Rev. Lett.* **2005**, *95*, 227402.

(4) Zhang, Y.; Grady, N. K.; Ayala-Orozco, C.; Halas, N. J. Three-dimensional nanostructures as highly efficient generators of second harmonic light. *Nano Lett.* **2011**, *11*, 5519−5523.

(5) Fan, W.; Zhang, S.; Panoiu, N.-C.; Abdenour, A.; Krishna, S.; Osgood, R. M.; Malloy, K. J.; Brueck, S. R. J. Second harmonic generation from a nanopatterned isotropic nonlinear material. *Nano Lett.* **2006**, *6*, 1027.

(6) Ginzburg, P.; Krasavin, A.; Zayats, A. V. Cascaded second-order surface plasmon solitons due to intrinsic metal nonlinearity. *New J. Phys.* **2013**, *15*, 013031.

(7) Boyd, R. W. *Nonlinear Optics*, 3rd ed.; Academic Press, 2008.

(8) Sipe, J. E.; Y.So, V. C.; Fukui, M.; Stegeman, G. I. Analysis of second-harmonic generation at metal surfaces. *Phys. Rev. B* **1980**, *21*, 4389.

(9) Dadap, J. I.; Shan, J.; Eisenthal, K. B.; Heinz, T. F. Second-harmonic Rayleigh scattering from a sphere of centrosymmetric material. *Phys. Rev. Lett.* **1999**, *83*, 4045−4048.

(10) Krausz, F.; Ivanov, M. Attosecond physics. *Rev. Mod. Phys.* **2009**, *81*, 163.

(11) Pletch, A.; Kotaidis, V.; Lotenc, M.; Boneberg, J. Femtosecond laser near-field ablation fromgold nanoparticles. *Nat. Phys.* **2006**, *2*, 44.

(12) Boyd, R. W.; Shi, Z.; De Leon, I. The third-order nonlinear optical susceptibility of gold. *Opt. Commun.* **2014**, *326*, 74−79.

(13) Dadap, J. I.; Shan, J.; Heinz, T. F. Theory of optical second-harmonic generation from a sphere of centrosymmetric material: small-particle limit. *J. Opt. Soc. Am. B* **2004**, *21*, 1328−1347.

(14) Makeev, E. V.; Skipetrov, S. E. Second harmonic generation in suspensions of spherical particles. *Opt. Commun.* **2003**, *224*, 139−147.

(15) Pavlyukh, Y.; Hubner, W. Nonlinear Mie scattering from spherical particles. *Phys. Rev. B* **2004**, *70*, 245434.

(16) Capretti, A.; Forestiere, C.; Dal Negro, L.; Miano, G. Full-wave analytical solution of second-harmonic generation in metal nanospheres. *Plasmonics* **2014**, *9*, 151−166.

(17) Bachelier, G.; Russier-Antoine, I.; Benichou, E.; Jonin, C.; Brevet, P.-F. Multipolar second-harmonic generation in noble metal nanoparticles. *J. Opt. Soc. Am. B* **2008**, *25*, 955−960.

(18) Ginzburg, P.; Hayat, A.; Berkovitch, N.; Orenstein, M. Nonlocal ponderomotive nonlinearity in plasmonics. *Opt. Lett.* **2010**, *35*, 1551−1553.

(19) Varró, S.; Ehlotzky, F. Higher-harmonic generation from a metal surface in a powerful laser field. *Phys. Rev. A* **1994**, *49*, 3106−3109.

(20) Farkas, Gy.; Tóth, Cs.; Moustaizis, S. D.; Papadogiannis, N. A.; Fotakis, C. Observation of multiple-harmonic radiation induced from a gold surface by picosecond neodymium-doped yttrium aluminum garnet laser pulses. *Phys. Rev. A* **1992**, *46*, R3605.
(21) Bohren, C. F.; Huffman, D. R. *Absorption and Scattering of Light by Small Particles*; Wiley VCH, 1998.
(22) Ginzburg, P.; Berkovitch, N.; Nevet, A.; Shor, I.; Orenstein, M. Resonances on-demand for plasmonic nano-particles. *Nano Lett.* **2011**, *11*, 2329−2333.
(23) Prodan, E.; Radloff, C.; Halas, N. J.; Nordlander, P. A. Hybridization model for the plasmon response of complex nanostructures. *Science* **2003**, *302*, 419−422.
(24) Ginzburg, P.; Krasavin, A.; Sonnefraud, S.; Murphy, A.; Pollard, R. J.; Maier, S. A.; Zayats, A. V. Nonlinearly coupled localized plasmon resonances: resonant second-harmonic generation. *Phys. Rev. B* **2012**, *86*, 085422.
(25) Berkovitch, N.; Ginzburg, P.; Orenstein, M. Nano-plasmonic antennas in the near infrared regime. *J. Phys.: Condens. Matter* **2012**, *24*, 073202.
(26) Ginzburg, P.; Zayats, A. V. Localized surface plasmon resonances in spatially dispersive nano-objects: phenomenological treatise. *ACS Nano* **2013**, *7*, 4334−4342.
(27) Scalora, M.; Vincenti, M. A.; de Ceglia, D.; Roppo, V.; Centini, M.; Akozbek, N.; Bloemer, M. J. Second- and third-harmonic generation in metal-based structures. *Phys. Rev. A* **2010**, *82*, 043828.
(28) Crouseilles, N.; Hervieux, P.-A.; Manfredi, G. Quantum hydrodynamic model for the nonlinear electron dynamics in thin metal films. *Phys. Rev. B* **2008**, *78*, 155412.
(29) Hurst, J.; Haas, F.; Manfredi, G.; Hervieux, P.-A. High-harmonic generation by nonlinear resonant excitation of surface plasmon modes in metallic nanoparticles. *Phys. Rev. B* **2014**, *89*, 161111(R).